Influence of multiple load indentation on the mechanical and material behaviour of steel cone-cylinder under axial compression

To cite this article: O Ifayefunmi *et al* 2021 *Mater. Res. Express* **8** 126504

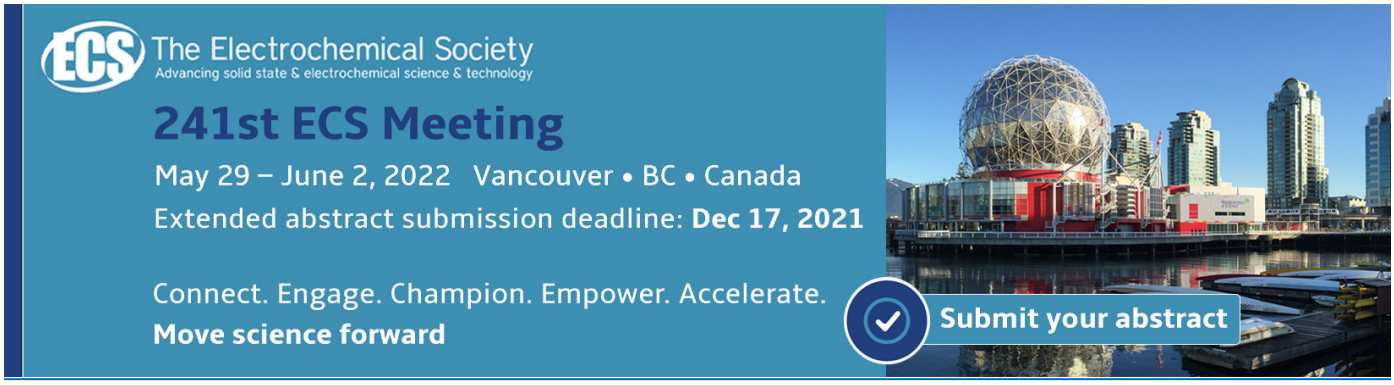

Materials Research Express

PAPER

Influence of multiple load indentation on the mechanical and material behaviour of steel cone-cylinder under axial compression

O Ifayefunmi[1,*], Sivakumar Dhar Malingam[2] and A H Sazali[1]

[1] Fakulti Teknologi Kejuruteraan Mekanikal Dan Pembuatan, Universiti Teknikal Malaysia Melaka, Hang Tuah Jaya, 76100 Durian, Tunggal, Melaka, Malaysia
[2] Centre for Advanced Research on Energy, Fakulti Kejuruteraan Mekanikal, Universiti Teknikal Malaysia Melaka, Hang Tuah Jaya, 76100, Durian Tunggal, Melaka, Malaysia
* Author to whom any correspondence should be addressed.

E-mail: olawale@utem.edu.my

Keywords: material behaviour, multiple load indentation, steel cone-cylinder, axial compression, buckling

OPEN ACCESS

RECEIVED
17 August 2021

REVISED
18 November 2021

ACCEPTED FOR PUBLICATION
22 November 2021

PUBLISHED
3 December 2021

Abstract

The first set of test data on axial collapse of cone-cylinder assembly having multiple load indentation (MLI) and its accompanying numerical studies is presented in this paper. Two perfect and two imperfect steel cone-cylinders were prepared in pairs. The cone-cylinder models have the following geometric parameters: cone radius of 40 mm, cylinder radius of 70 mm,wall thickness of 0.5 mm and cone angle of 16.7°. Cone and cylinder part were combined using Metal Inert Gas (MIG) welding technique. Results show that the repeatability of the experiment was good (3% for the perfect and 7% for the imperfect). Also, numerical prediction tends to reproduce the test data with good accuracy. The error between both approches ranges from 1% to −8%. Furthermore, the influence of geometric parameters are also significant in determining the collapse load of this type of structure. Finally, the worst multiple load indentation (WMLI) was explored for steel cone-cylinders assembly using different number of load indentations. Results indicate that as the number of indents increases, the sensitivity of the cone-cylinder models to imperfection also increases. However, at different imperfection amplitude, A, two regions were observed; (i) the region where cone-cylinder with $N = 8$ is more sensitive ($A < 1.5$), and (ii) the region where $N = 4$ produce the worst imperfection ($1.5 < A \leqslant 1.68$).

1. Introduction

The major difference between the theoretical calculations and experimental results for thin-walled shell structures in the past has been said to be as a result of initial geometric imperfections. Expectedly, because the stress on the structure is confined to the location of the imperfection, the failure of the structure is restricted to this region. Thereby, resulting in the reduction of the structural stability of the structure. This has sprawned up significant interest in the study of imperfection sensitivity of such structures. Review of research on the effect of imperfection on cones and/or cylinders under different loads is presented in [1, 2]. While, reference [1] is devoted to cones or cylinder, [2] on the other hand, concentrate on cone and cylinder assembly. More recently, the Load Indentation imperfection approach is gaining more attention as one of the most practical approach for producing imperfection on the shell structures. Many researchers have employed this approach both experimentally and numerically to simulate imperfection on different thin-walled shell made from steel or composite structures. As an example, the single load indentation (SLI) imperfection was applied on cylindrical shells in [3–8], conical shell structures in [9–16] and domes in [17, 18].

Thin-walled structure having cone and cylinder combination is not an exception. In fact, it is generally believed that the presence of imperfections on combination of cone and cylinder structures can greatly reduce the buckling load of such structures. References to numerical investigations on the impact of initial geometric defects on the instability of cone and cylinder assembly can be found in [19–21]. Reference [19] was devoted to

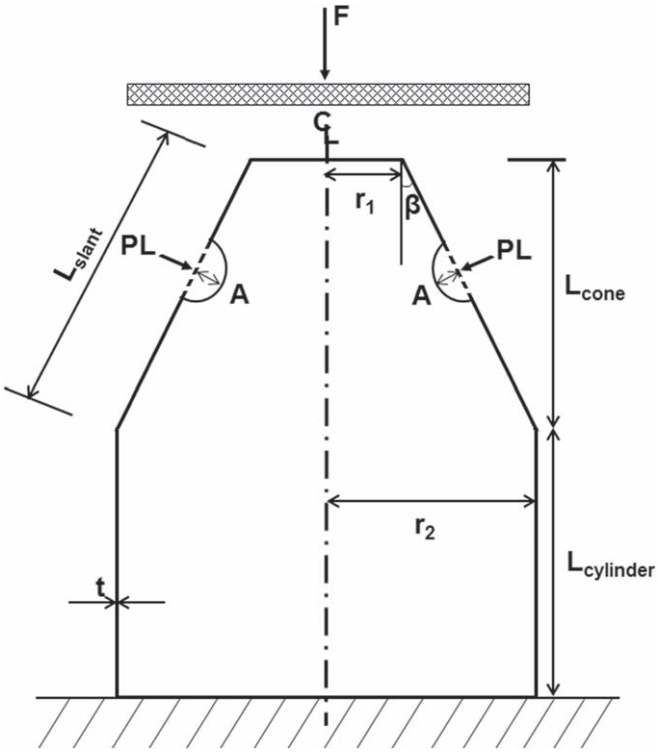

Figure 1. Illustration of cone-cylinder model having multiple load indentation.

the influence of Axisymmetric outward bulge, Eigenmode and Single Load Indentation imperfections on the failure of unstiffened cylinder-cone-cylinder combination under axial compression. While, [20] on the other hand covers the influence of Eigenmode and Single Load Indentation imperfections on the structural failure of unstiffened cone-cylinder assembly under external pressure. Investigation on internally pressurized imperfect ring-stiffened cone and cylinder combination was presented in [21]. The imperfection was affined to geometric shape imperfections. More recently, reference [22] presents the first experiemental data on axially compressed cone-cylinder models with SLI imperfection. However, question arises on the suitability of SLI imperfection to produce the worst imperfection scenario or its appropriateness for design purposes. Hence, the need for a more robust approach to determine the worst imperfection behavior such as the worst multiple load indentation (WMLI). References on the WMLI approach can be found in [23–25] for cylindrical shells and [9, 26] for conical shells.

To date, it is shocking that there is little or no information on collapse test data for axially compressed cone-cylinder assembly having initial geometric defect in the form of multiple load indentation. This paper aims to provide the first experimental data on the consequences of MLI imperfection on the instability of steel cone-cylinder assembly under axial compressive load. Four steel cone-cylinders having radius-to-thickness ratio, r1/t, of 80 were manufactured and tested under axial compression. First, ABAQUS FE code [27] were used to benchmark the experimental data. Next, extensive numerical computations were implemented to explore the effect of cone- cylinder geometry such as r1/t and cone angle. Finally, the worst multiple load indentation approach is presented.

2. Methodology

2.1. Manufacturing method and material

Four cone-cylinder specimens were fabricated in pairs from 0.5 mm steel plate employing the traditional manufacturing process. The first two samples were perfect shells with no indent, while multiple (2) local indents having nominal indentation amplitudes of 0.56 were introduced in the remaining two specimens. The cone-cylinders were produced in pairs to confirm the replicability of the test data. The nominal geometric parameters of the cone-cylinder specimens are: cone radius, $r_1 = 40$ mm, cylinder radius, $r_2 = 70$ mm, wall thickness, $t = 0.5$ mm, cone length, $L_{cone} = 100$ mm, cylinder length, $L_{cylinder} = 100$ mm and cone angle, β of 16.7°. The models were identified as Specimen 1–4. Axial load, F and local indentation force, PL, were applied on all the cone-cylinder models as illustrated in figure 1. The indentation load is applied at two opposite position on the

Table 1. Cone-cylinder models measured thickness.

Specimen	N	t_{min}	t_{max} (mm)	t_{ave}	t_{std}
1	0	0.48	0.49	0.49	0.005
2	0	0.47	0.49	0.48	0.004
3	2	0.48	0.50	0.48	0.005
4	2	0.48	0.50	0.49	0.006

Table 2. Cone-cylinder models measured geometric data.

Specimen	N	$2r_1$	$2r_2$	L (mm)	L_{slant}	$\beta(^\circ)$
1	0	80.14	139.97	200.39	105.01	16.6
2	0	80.22	140.14	200.10	105.08	16.6
3	2	80.80	139.10	200.18	105.07	16.6
4	2	80.45	139.80	200.38	104.23	16.6

Figure 2. Typical photograph of cone-cylinder specimen testing arrangement using SHIMADZU universal Testing Machine.

circumferential axis of the cone-cylinder to produce indents having desired indentation amplitude, A - see figure 1.

To fabricate the cone-cylinder model, different manufacturing process were employed ranging from cutting, cold rolling, and welding. First, conical and cylindrical samples were cut separately using the laser jet cutting machine. Next, the individual cones and cylinders were rolled into shape using conventional rolling machine. The feed controller of the rolling machine were regulated to produce the conical or cylindrical shape. Then, Metal Inert Gas (MIG) welding process was employed to join the longitudinal seams of the cones and cylinders. After producing individual cones and cylinders, the enclosed edge of the cone big radius end is joined to the cylinder. To introduce the 0.56 mm indentations on the imperfect specimens (Specimens 3 and 4), pressure load was applied to the cone-cylinder model manually from a vertical milling machine. The quill feed of the machine was lowered down gradually until the indentation having an approximate imperfection amplitude was formed. This process was repeated at the opposite location of the first dent. Although, it must be mentioned that for multiple dimple it is practically impossible to maintain the desired indentation magnitude on both side of the

Table 3. Load carrying capacity of cone-cylinders assembly under axial collapse test. Expl = experimental, Num = Numerical.

Specimen	Imperfection amplitude (mm)		Collapse load (kN)		Expl/Num
	Nominal	Measured	Expl	Num	
1	0	0	14.4618	14.3491	1.01
2	0	0	14.0056	14.162	0.99
3	0.56	0.56/0.71	13.2596	14.3561	0.92
4	0.56	0.81/0.60	14.2928	14.2817	1.00

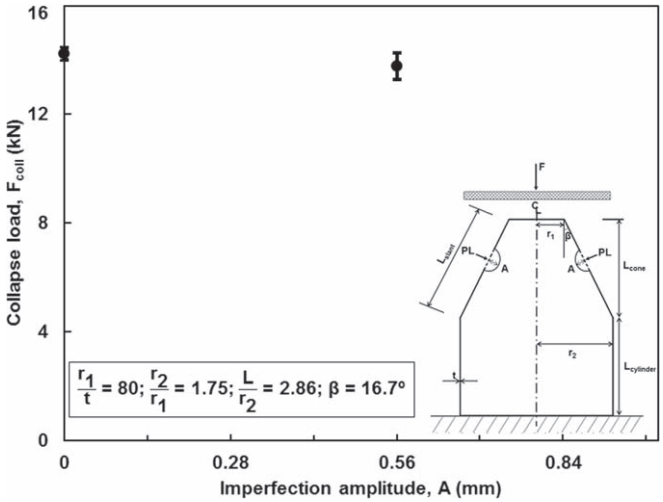

Figure 3. Plot of average experimental collapse force against indentation amplitude, A, for cone-cylinder assembly having r1/t of 80.

specimen using the manual pressure application. The indents were initiated half way through the cone's slant length. The choice of the location of the indent bored out by [19], where cylinder-cone-cylinder transition under axial compression with indentation at the cone's mid-length was seen to be more sensitive to imperfection as compared to other locations. More details about the specimens fabrication process, the local indentation process and the clamping arrangement during the indentation process can be found in [22].

JIS G 3141 mild steel was used to produce the cone-cylinder models. To extract the actual material data for the models, uni-axial tensile test based on the British Standards [28] was carried out at the speed of 1 mm/min. The average material data obtained from the uni-axial test are as follows: Yield stress, $\sigma yp = 167.309$ MPa, Young's modulus, $E = 190.927$ GPa and Poisson's ratio, $\nu = 0.3$. To note, this material properties will be employed for numerical computations in section 3.

2.2. Axial collapse test

Prior to axial collapse test of the manufactured specimens using Shimadzu universal testing machine. Several measurements of the cone-cylinders were taken prior to the axial collapse test. Table 1 summarized the measurement data for the cone-cylinders' thickness and table 2 presents the measurement data for the cone-cylinders' geometrical parameters (e.g., diameters, lengths and cone angle), where N = number of load indentation. First, thickness measurement were carried out using a micrometer screw gauge at 22 (circumferential) x 22 (longitudinal) points on the cone-cylinder surface. Next, the cone-cylinder's top and bottom diameters and the cone slant length were measured with a Vernier caliper. Then, digital height gauge was utilized to measure the axial height of each specimen. Additionally, to measure the depth of indentations, a Vernier calliper was employed and the ensuing measured data is given in column 4 of table 3.

Expectedly, variation in the measured indentation amplitude for specimens 3 and 4 was observed. This is because the local indentation were applied manually and it is practically hard to acquire the same indentation amplitude on both side of the cone-cylinder. Finally, the specimens were collapse using an incremental axial load (1 mm min^{-1}) through an Shimadzu universal testing machine. The top and bottom edges of the cone-cylinders were covered with plates to constrain both displacement and rotational movement during the experiment as photographed in figure 2 for a typical cone-cylinder specimen ready for testing. It is expected that this will

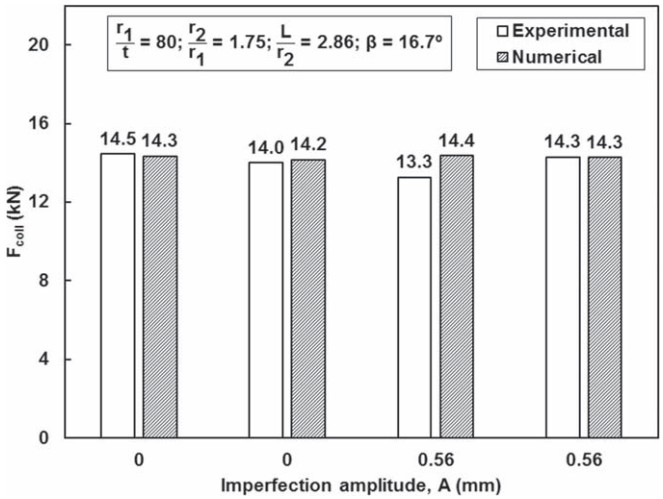

Figure 4. Comparison of collapse load from experiments and simulations for all tested cone-cylinder assembly.

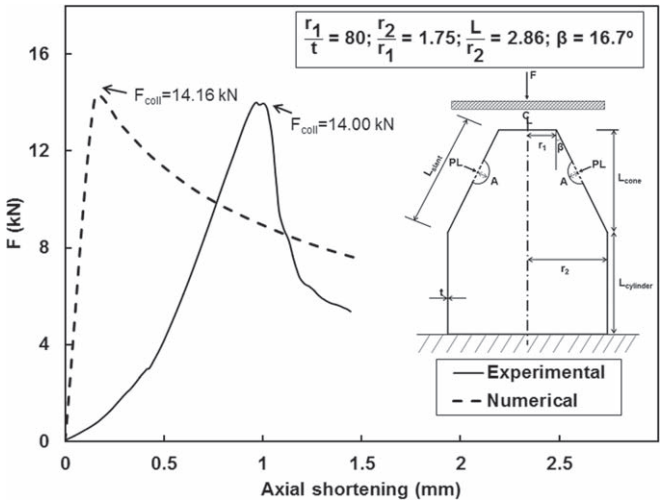

Figure 5. Typical graph of experimental and numerical load versus axial shortening for cone-cylinder assembly (perfect model - Specimen 2).

provide the assummed experimental boundary condition (i.e., fixed condition at the bottom end of the model, while only axial movement is allowed at the top end).

3. Results and discussion

This section present the test data acquired from the axial collapse test and its accompanying numerical results. First, experimental axial collapse force for all the tested samples are provided. Figure 3 depicts the plot of average experimental collapse load versus imperfection amplitude with an error bar indicating error margin in each pairs. The exact size of failure load for all tested cone-cylinder models is presented in table 3.

It is apparent that there is good repeatabily of test data with error ranging from 1% (for perfect cone-cylinder shells) to 8% (for imperfect models). The large error experienced for imperfect cone-cylinder models can be attributed to the non-uniformity of local indentation amplitude during the manufacturing process - see measured indentation amplitude in column 4 of table 3.

Next, ABAQUS FE code was employed to validate the experimental data. The numerical calculations utilized the average measured data of the models (see tables 1 and 2), measured indentation amplitude (see column 4 of table 3) and the material properties acquired through uni-axial test as provided in section 2.1. ABAQUS S4R shell element was used to modeled the cone-cylinder specimen. To reproduce the test set-up, both the top and bottom edge of the cone-cylinder models were covered with undeformable plates. The interaction between the nodes at the top cone edge and the inner surface of the undeformable plate was assummed to be surface-to-

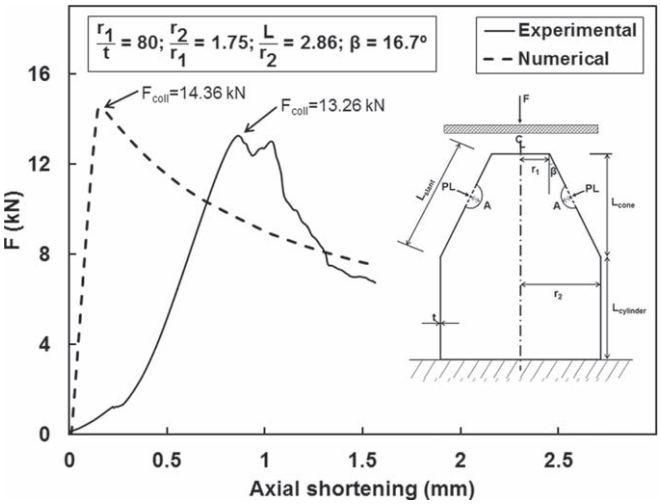

Figure 6. Typical graph of experimental and numerical load against axial shortening for cone-cylinder model with multiple indent (Specimen 3).

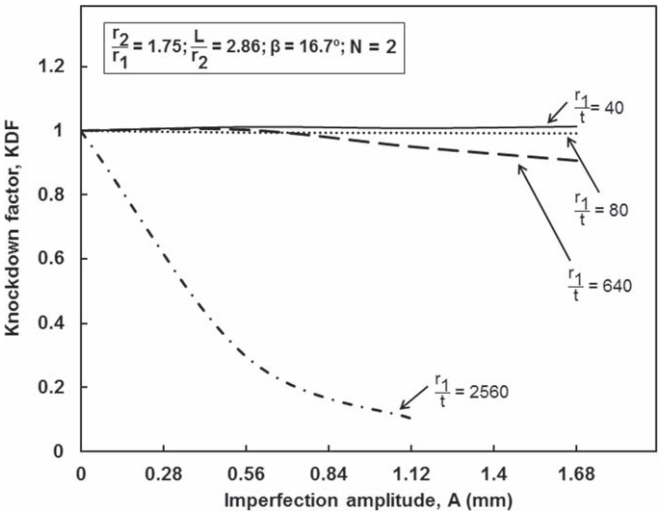

Figure 7. Plot of normalized axial force against indentation amplitude for imperfect cone-cylinder models with multiple indent, N = 2, with different thinness ratios.

surface contact interaction with frictionless tangential behavior. Since the impact of weld area on the failure load of pressure hulls [29] and cone-cylinders [30] is said to be marginally. During the numerical simulation, the weld area of the cone-cylinder transition was ignored from the modeling. The cylindrical end of the structure is assumed to be fixed, while only axial movement is permited at the conical end. To simulate the local indentation, perturbation load was applied to the conical portion, half-way through its slant length. To run the analysis, two different steps were involved, they are: (i) static general procedure - to simulate the local indent of the desired amplitude, and (ii) static Riks analysis - to apply axially compressed load on the specimen until failure. Figure 4 depicts the plot of comparison of experimental and numerical collapse load versus indentation amplitude for all cone-cylinder assembly subjected to axial collapse test. The failure load resulting from the numerical computation of cone-cylinder specimens are given in column 6 of table 3. From figure 4, it is apparent that the numerical collapse load of cone-cylinder shells reproduce the experimental counterpart with good accuracy. The errors between experimental to numerical collapse load were 1% (for specimen 1), 1% (for specimen 2), 8% (for specimen 3), and 0% (for specimen 4). Again, it can be said that experimental and numerical collapse load for perfect cone-cylinder model produce a better agreement as compared to its imperfect counterpart.

Typical graphs of comparison between experimental and numerical load versus axial shortening for perfect cone-cylinder model (specimen 2) and imperfect cone-cylinder specimen with local indentation (specimen 3) can be found in figures 5 and 6, respectively. From both Figures, it can be observed that the load versus axial

Table 4. Collapse force (kN) of cone-cylinder assembly (perfect and imperfect) with different thinness ratio, r_1/t.

Top radius-to-thickness ratio, r_1/t	Imperfection amplitude, A (mm)			
	0	0.56	1.12	1.68
40	35.873	36.300	36.147	36.323
80	14.825	14.746	14.736	14.710
640	0.864	0.866	0.821	0.783
2560	0.232	0.069	0.024	—

Table 5. Collapse load (kN) of cone-cylinder models having different cone angle, β.

Indentation amplitude, A	Cone angle, β (°)			
	5	10	15	20
0	26.257	20.072	16.218	13.560
0.56	26.215	20.070	16.172	13.474
1.12	26.088	19.975	16.134	13.414
1.68	25.756	19.827	16.068	13.303

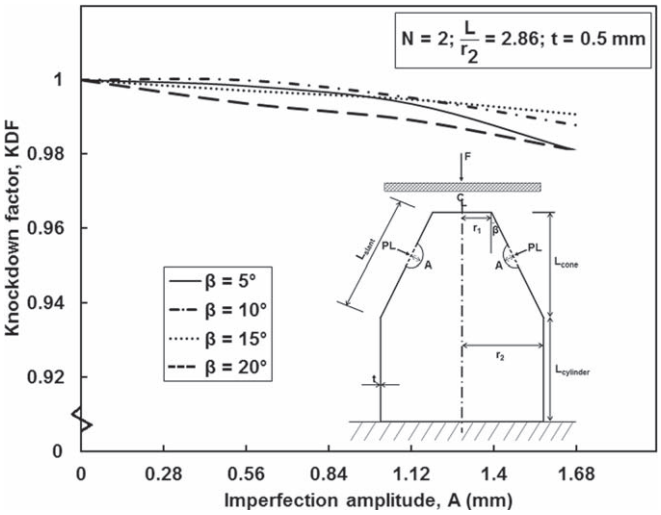

Figure 8. Plot of normalized axial force against indentation amplitude for imperfect cone-cylinder models with multiple indent, N = 2, having different cone angle.

shortening plot is nearly linear up to collapse load. After which the failure load of the structure drops smoothly within the post-collapse dormain.

Again, it can be seen that both the experimental and numerical plots observe the same pre collapse and post-collapse paths. Although, it must be mentioned that the experimental curves are less stiffner as compared to the numerical curves. This appears to be a common trend and has previously been ascribed to material behaviour adopted in the finite element simulations [10]. It is expected that using plastic material behavior with linear strain hardening will produce a better agreement. In addition, the use explicit dynamics analysis may provide a better trend of the load versus axial shortening plot between experiment and finite element analysis.

Then, further finite element computations were carried out to investigate the effect of cone-cylinder geometry such as (i) thinness ratio, r_1/t, and (ii) cone semi-vertex angle, β, on the structural instability of cone-cylinder transition under axial compression. The analysis modelling and procedure were the same as discussed previously. To achieve different r_1/t, of 40, 80, 640 and 2560, the small radius end of the cone-cylinder model, r1, is kept constant at 40 mm, and the wall thickness, t, is assumed to be varied. Figure 7 depicts the curve of knockdown factor against indentation amplitude for imperfect cone-cylinder models with multiple indent, N = 2, having different radius-to-thickness ratios. To note, the knockdown factor is the ratio of imperfect collapse load to the perfect collapse load for each cases considered. The corresponding magnitude of failure load for cone-cylinders (perfect and imperfect) with different r_1/t is given in table 4. It is obvious that increasing the

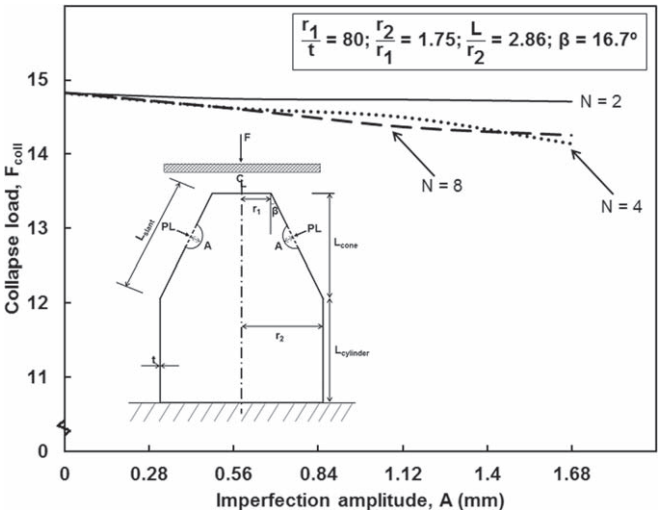

Figure 9. Plot of failure load against indentation amplitude for cone-cylinder with $r_1/t = 80$ and different number of indents.

Table 6. Collapse load (kN) for cone-cylinder assembly (perfect and imperfect) having r_1/t of 80 and different number of load indentation, N.

Indentation amplitude, A	Number of load indentations, N			
	1	2	4	8
0	14.825 (1.00)	14.825 (1.00)	14.825 (1.00)	14.825 (1.00)
0.56	14.793 (0.998)	14.746 (0.995)	14.624 (0.986)	14.613 (0.985)
1.12	14.781 (0.997)	14.736 (0.994)	14.503 (0.978)	14.368 (0.969)
1.68	14.710 (0.992)	14.710 (0.992)	14.145 (0.954)	14.255 (0.961)

cone-cylinder indentation amplitude, results in a decrease in the failure load of the structures. This behaviour is more pronouced as the r_1/t of the cone-cylinder increases. This implies that relatively thick cone-cylinder structures with low r_1/t, is less sensitive to multiple indent imperfection as compared to thinner cone-cylinder models with high r_1/t.

To investigate the influence of cone angle of the instability behaviour of the cone-cylinder specimens under axial compression, the big radius ends of the cone-cylinder is kept constant, whereas the small radius edge of the structure is varied. The cone angles considered in this paper are 5°, 10°, 15° and 20°. Table 5 presents the ensuing numerical collapse load for cone-cylinder model with multiple indent, $N = 2$ having different cone angle.

Figure 8 on the other hand depicts the graph of collapse load against indentation amplitude for imperfect cone-cylinder models with multiple indent, $N = 2$, having different cone angle. Again, it can be seen that as the cone angle of the cone-cylinder increase, the sensitivity of the cone-cylinder structures to multiple indentation increases. This result is in agreement with that of [12, 16] for conical shells under axial compressive load.

Lastly, numerical calculations were conducted to investigate the worst multiple load indentation (WMLI) for cone-cylinder specimens subjected to axial compression with indentation amplitude, A, ranging between 0.28 and 1.68. The number of indent, N, on the cone-cylinder model was within the range of 1 and 8. Cone-cylinder shell with $r_1/t = 80$ is considered here. Table 6 gives the collapse load for cone-cylinder shells with different indentation amplitude having different number of indents. The number in parenthesis correspond to the ratio of imperfect collapse load to perfect collapse load. From table 6, axially compressed imperfect steel cone-cylinder shells with multiple load indentation (MLI) are seen to be more sensitive as compared to cone-cylinder model with single load indentation (SLI). This is consistent with the result of [9] for composite cones, [31] for composite cylinders and [23] for aluminium alloy cylinders. Figure 9 depicts the plot of collapse load versus indentation amplitude for cone-cylinder with different number of indents. Again, it is apparent that as the number of indents increases, the sensitivity of the cone-cylinder models to imperfection also increases. However, two regions were observed; (i) the region where cone-cylinder with $N = 8$ is more sensitive, and (ii) the region where $N = 4$ produce the worst imperfection. As an example, for cone-cylinder specimen with indentation amplitude, $A < 1.5$, the model with $N = 8$ produce the lowest load carrying capacity for the structure. Moreover, going beyond this point i.e., $1.5 < A \leqslant 1.68$, cone-cylinder model with $N = 4$ appears to be more sensitivity. This trend was also observed for axially compressed steel cone where specimens with 2

multiple load indentation (two indents) produce the worst sensitivity thereby producing the worst multiple load indentation (WMLI) for indentation amplitude, $0.28 < A \leqslant 1.68$. However, for $A \leqslant 0.28$, 4 multiple load indentation (four indents) provides the worst result [26]. Surprisingly, the behaviour is a bit different from that of axially compressed stiffened composite conical shells where specimens with 6 load indentations were reported to produce the worst sensitivity thereby producing the WMLI for the structure [9]. It can be said here that the influence of material behaviour is important. Although this may not be generally true. Hence further work on the influence of material behaviour and optimal number of indents to produce the worst multiple load indentation is desirable.

4. Conclusions

The load indentation imperfection approach has been successfully applied to steel cone-cylinder models both experimentally and numerically. Repeatability of experimental axial collapse test on cone-cylinder shells with or without multiple local indent was good. Numerically computed collapse load was seen to reproduce its experimental counterpart with a fair margin. From the aforementioned results, the ensuing conclusions can be drawn: (i) both experiment and simulation results indicates that the presence of local indentation imperfection can significantly influence the failure load of the cone-cylinder structures, (ii) axially compressed steel cone-cylinder assembly having multiple load indentation (MLI) imperfection is more sensitive to imperfection as compared to cone-cylinder model with single load indentation (SLI) imperfection, and (iii) for steel cone-cylinder under axial compression, increasing the number of indent tends to increase the sensitivity of the structure to imperfection. Although, the optimum number of indents is not clear since there is transition between $N = 8$ and $N = 4$ depending on the indentation amplitude.

Acknowledgments

Special thanks to the Universiti Teknikal Malaysia Melaka (UTeM) for the financial assistant acquired under Journal Incentive Grant Scheme JURNAL/2020/FTKMP/Q00052. Also, the authors will like to thank Miss. Fairuz Mardhiah Mahidan for her help to carry out the analysis.

Data availability statement

All data that support the findings of this study are included within the article (and any supplementary files).

ORCID iDs

O Ifayefunmi https://orcid.org/0000-0002-9527-325X
Sivakumar Dhar Malingam https://orcid.org/0000-0001-7968-1950

References

[1] Ifayefunmi O and Błachut J 2018 Imperfection sensitivity: a review of buckling behavior of cones, cylinders, and domes *Journal of Pressure Vessel Technology, Transactions of the ASME* **140** 050801
[2] Ifayefunmi O and Ismail M S 2020 An overview of buckling and imperfection of cone-cylinder transition under various loading condition *Latin American Journal of Solids and Structures* **17** 1–21
[3] Arbelo M, Zimmermann R, Castro S and Degenhardt R 2013 Comparison of new design guidelines for composite cylindrical shells prone to buckling *Int. Conf. on Computational Science and Technology, (24-26 April), 96–111. Sorrento, Italy*
[4] Castro S G P, Zimmermann R, Arbelo M A and Degenhardt R 2013 Exploring the constancy of the global buckling load after a critical geometric imperfection level in thin-walled cylindrical shells for less conservative knock-down factors *Thin Walled Struct.* **72** 76–87
[5] Ghanbari Ghazijahani T, Jiao H and Holloway D 2014 Experiments on dented cylindrical shells under peripheral pressure *Thin-Walled Structures* **84** 50–8
[6] Khakimova R, Castro S G P, Wilckens D, Rohwer K and Degenhardt R 2017 Buckling of axially compressed CFRP cylinders with and without additional lateral load : Experimental and numerical investigation *Thin-Walled Structures* **119** 178–89
[7] Orifici A C and Bisagni C 2013 Perturbation-based imperfection analysis for composite cylindrical shells buckling in compression *Compos. Struct.* **106** 520–8
[8] Wagner H N R, Hühne C, Niemann S and Khakimova R 2017 Robust design criterion for axially loaded cylindrical shells - simulation and validation *Thin-Walled Structures* **115** 154–62
[9] Hao P, Wang B, Du K, Li G, Tian K, Sun Y and Ma Y 2016 Imperfection-insensitive design of stiffened conical shells based on equivalent multiple perturbation load approach *Compos. Struct.* **136** 405–13
[10] Ifayefunmi O and Mahidan F M 2021 Collapse of conical shells having single dimple imperfection under axial compression *Journal of Pressure Vessel Technology, Transactions of the ASME* **143** 1–8

[11] Khakimova R, Warren C J, Zimmermann R, Castro S G P, Arbelo M A and Degenhardt R 2014 The single perturbation load approach applied to imperfection sensitive conical composite structures *Thin-Walled Structures* **84** 369–77
[12] Khakimova R, Wilckens D, Reichardt J, Zimmermann R and Degenhardt R 2016 Buckling of axially compressed CFRP truncated cones: Experimental and numerical investigation *Compos. Struct.* **146** 232–47
[13] Wagner H N R, Hühne C and Khakimova R 2018 Towards robust knockdown factors for the design of conical shells under axial compression *Int. J. Mech. Sci.* **146–147** 60–80
[14] Castro S G P, Mittelstedt C, Monteiro F A C, Degenhardt R and Ziegmann G 2015 Evaluation of non-linear buckling loads of geometrically imperfect composite cylinders and cones with the Ritz method *Compos. Struct.* **122** 284–99
[15] Ghanbari Ghazijahani T, Jiao H and Holloway D 2015 Experiments on locally dented conical shells under axial compression *Steel and Composite Structures* **19** 1355–67
[16] Özyurt E, Yilmaz H and Tomek P 2017 Prediction of the influence of geometrical imperfection to load carrying capacity of conical shells under axial loading *Sigma Journal of Engineering and Natural Sciences* **36** 11–20
[17] Blachut J 2020 Impact of local and global shape imperfections on buckling of externally pressurised domes *Int. J. Press. Vessels Pip.* **188** 104178
[18] Blachut J 2016 Buckling of composite domes with localised imperfections and subjected to external pressure *Compos. Struct.* **153** 746–54
[19] Ismail M S, Ifayefunmi O and Fadzullah S H S M 2019 Buckling of imperfect cylinder-cone-cylinder transition under axial compression *Thin-Walled Structures* **144** 106250
[20] Ismail M S, Ifayefunmi O, Fadzullah S H S M and Johar M 2020 Buckling of imperfect cone-cylinder transition subjected to external pressure *Int. J. Press. Vessels Pip.* **187** 104173
[21] Zhao Y 2005 Buckling behaviour of imperfect ring-stiffened cone—cylinder intersections under internal pressure *Int. J. Press. Vessels Pip.* **82** 553–64
[22] Ifayefunmi O and Mahidan F M 2021 Collapse of cone-cylinder transitions having single load indentation imperfection subjected to axial compression *Int. J. Press. Vessels Pip.* A **194** 104506
[23] Hao P, Wang B, Li G, Meng Z, Tian K, Zeng D and Tang X 2014 Worst multiple perturbation load approach of stiffened shells with and without cutouts for improved knockdown factors *Thin-Walled Structures* **82** 321–30
[24] Hao P, Wang B, Tian K, Du K and Zhang X 2015 Influence of imperfection distributions for cylindrical stiffened shells with weld lands *Thin-Walled Structures* **93** 177–87
[25] Wang B, Du K, Hao P, Tian K, Chao Y J, Jiang L, Xu S and Zhang X 2019 Experimental validation of cylindrical shells under axial compression for improved knockdown factors *Int. J. Solids Struct.* **164** 37–51
[26] Ifayefunmi O, Mahidan F M and Maslan M H 2020 Instability of conical shells with multiple dimples under axial compression *International Journal of Recent Technology and Engineering* **8** 1022–7
[27] Hibbit K and Sorensen I 2006 *ABAQUS—Theory and Standard User's Manual Version 6.3. Hibbit* (Pawtucket, RI: Karlsson and Sorensen)
[28] BSI 2001 *Tensile Testing Off Metallic Materials, Part (1), Method of Test at Ambient Temperature.* (London: British Standard Institute) Standard No. BS EN 10002–1
[29] Gannon L 2010 Prediction of the effects of cold bending on submarine pressure hull collapse *Technical Memorandum* (Atlantic, TM: DRDC) 2010-065
[30] Ismail M S, Ifayefunmi O and Mazli A H 2020 Combined stability of cone-cylinder transition subjected to axial compression and external pressure *Thin-Walled Structures* **157** 1–14
[31] Arbelo M, Degenhardt R, Castro S G P and Zimmermann R 2014 Numerical characterization of imperfection sensitive composite structures *Compos. Struct.* **108** 295–303